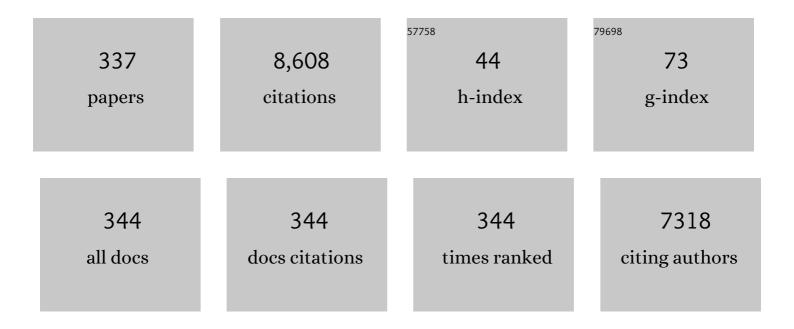
List of Publications by Year in descending order

Source: https://exaly.com/author-pdf/1255293/publications.pdf Version: 2024-02-01



PALE MOOS

#	Article	IF	CITATIONS
1	Defect Chemistry of Donorâ€Doped and Undoped Strontium Titanate Ceramics between 1000° and 1400°C. Journal of the American Ceramic Society, 1997, 80, 2549-2562.	3.8	482
2	Metal-Organic Frameworks for Sensing Applications in the Gas Phase. Sensors, 2009, 9, 1574-1589.	3.8	377
3	Electronic transport properties of Sr1â^'xLaxTiO3ceramics. Journal of Applied Physics, 1996, 80, 393-400.	2.5	204
4	Selective ammonia exhaust gas sensor for automotive applications. Sensors and Actuators B: Chemical, 2002, 83, 181-189.	7.8	192
5	A Brief Overview on Automotive Exhaust Gas Sensors Based on Electroceramics. International Journal of Applied Ceramic Technology, 2005, 2, 401-413.	2.1	179
6	Why does the electrical conductivity in PEDOT:PSS decrease with PSS content? A study combining thermoelectric measurements with impedance spectroscopy. Journal of Polymer Science, Part B: Polymer Physics, 2012, 50, 976-983.	2.1	162
7	Solid State Gas Sensor Research in Germany – a Status Report. Sensors, 2009, 9, 4323-4365.	3.8	134
8	Hall mobility of undoped n-type conducting strontium titanate single crystals between 19 K and 1373 K. Applied Physics A: Materials Science and Processing, 1995, 61, 389-395.	2.3	132
9	Zeolites — Versatile materials for gas sensors. Solid State Ionics, 2008, 179, 2416-2423.	2.7	129
10	Materials for temperature independent resistive oxygen sensors for combustion exhaust gas control. Sensors and Actuators B: Chemical, 2000, 67, 178-183.	7.8	127
11	Sulfur Removal from Lowâ€6ulfur Gasoline and Diesel Fuel by Metalâ€Organic Frameworks. Chemical Engineering and Technology, 2010, 33, 275-280.	1.5	121
12	Thermopower of Sr1â^'xLaxTiO3ceramics. Journal of Applied Physics, 1995, 78, 5042-5047.	2.5	109
13	Selective mixed potential ammonia exhaust gas sensor. Sensors and Actuators B: Chemical, 2009, 140, 585-590.	7.8	103
14	Resistive Oxygen Gas Sensors for Harsh Environments. Sensors, 2011, 11, 3439-3465.	3.8	91
15	Textured PMN–PT and PMN–PZT. Journal of the American Ceramic Society, 2008, 91, 929-933.	3.8	90
16	Temperature-independent resistive oxygen exhaust gas sensor for lean-burn engines in thick-film technology. Sensors and Actuators B: Chemical, 2003, 93, 43-50.	7.8	89
17	Hydrocarbon sensing with thick and thin film p-type conducting perovskite materials. Sensors and Actuators B: Chemical, 2005, 108, 102-112.	7.8	85
18	Development and working principle of an ammonia gas sensor based on a refined model for solvate supported proton transport in zeolites. Physical Chemistry Chemical Physics, 2003, 5, 5195-5198.	2.8	84

#	Article	IF	CITATIONS
19	Solubility of lanthanum in strontium titanate in oxygen-rich atmospheres. Journal of Materials Science, 1997, 32, 4247-4252.	3.7	82
20	Catalysts as Sensors—A Promising Novel Approach in Automotive Exhaust Gas Aftertreatment. Sensors, 2010, 10, 6773-6787.	3.8	71
21	Formation and Effect of NH ₄ ⁺ Intermediates in NH ₃ –SCR over Fe-ZSM-5 Zeolite Catalysts. ACS Catalysis, 2016, 6, 7696-7700.	11.2	68
22	Influence of Carrier Gas Composition on the Stress of Al2O3 Coatings Prepared by the Aerosol Deposition Method. Materials, 2014, 7, 5633-5642.	2.9	62
23	Planar Microstrip Ring Resonators for Microwave-Based Gas Sensing: Design Aspects and Initial Transducers for Humidity and Ammonia Sensing. Sensors, 2017, 17, 2422.	3.8	62
24	Direct Catalyst Monitoring by Electrical Means: An Overview on Promising Novel Principles. Topics in Catalysis, 2009, 52, 2035-2040.	2.8	58
25	Selective impedance based gas sensors for hydrocarbons using ZSM-5 zeolite films with chromium(III)oxide interface. Sensors and Actuators B: Chemical, 2006, 119, 441-448.	7.8	56
26	Characterization of nickel manganite NTC thermistor films prepared by aerosol deposition at room temperature. Journal of the European Ceramic Society, 2018, 38, 613-619.	5.7	56
27	Powder requirements for aerosol deposition of alumina films. Advanced Powder Technology, 2015, 26, 1143-1151.	4.1	55
28	Ceramic meso hot-plates for gas sensors. Sensors and Actuators B: Chemical, 2004, 103, 91-97.	7.8	54
29	Assessment of the novel aerosol deposition method for room temperature preparation of metal oxide gas sensor films. Sensors and Actuators B: Chemical, 2009, 139, 394-399.	7.8	54
30	On the Electrochemical CO ₂ Reduction at Copper Sheet Electrodes with Enhanced Long-Term Stability by Pulsed Electrolysis. Journal of the Electrochemical Society, 2018, 165, J3059-J3068.	2.9	53
31	Direct thermoelectric gas sensors: Design aspects and first gas sensors. Sensors and Actuators B: Chemical, 2007, 123, 413-419.	7.8	52
32	Application of V2O5/WO3/TiO2 for Resistive-Type SO2 Sensors. Sensors, 2011, 11, 2982-2991.	3.8	52
33	Dual Mode NOx Sensor: Measuring Both the Accumulated Amount and Instantaneous Level at Low Concentrations. Sensors, 2012, 12, 2831-2850.	3.8	52
34	Chemically synthesized one-dimensional zinc oxide nanorods for ethanol sensing. Sensors and Actuators B: Chemical, 2013, 187, 295-300.	7.8	52
35	Sensing the soot load in automotive diesel particulate filters by microwave methods. Measurement Science and Technology, 2010, 21, 035108.	2.6	50
36	Influence of the V2O5 content of the catalyst layer of a non-Nernstian NH3 sensor. Solid State Ionics, 2014, 262, 270-273.	2.7	50

#	Article	IF	CITATIONS
37	Exploiting Synergies in Catalysis and Gas Sensing using Noble Metal‣oaded Oxide Composites. ChemCatChem, 2018, 10, 864-880.	3.7	50
38	Dense Y-doped ion conducting perovskite films of BaZrO3, BaSnO3, and BaCeO3 for SOFC applications produced by powder aerosol deposition at room temperature. International Journal of Hydrogen Energy, 2020, 45, 10000-10016.	7.1	50
39	Hot Plate Gas Sensors-Are Ceramics Better?. International Journal of Applied Ceramic Technology, 2005, 2, 383-389.	2.1	48
40	Method for detection of NO in exhaust gases by pulsed discharge measurements using standard zirconia-based lambda sensors. Sensors and Actuators B: Chemical, 2010, 147, 780-785.	7.8	47
41	Investigation of the electrode effects in mixed potential type ammonia exhaust gas sensors. Solid State Ionics, 2011, 192, 38-41.	2.7	47
42	A Laboratory Test Setup for in Situ Measurements of the Dielectric Properties of Catalyst Powder Samples under Reaction Conditions by Microwave Cavity Perturbation: Set up and Initial Tests. Sensors, 2014, 14, 16856-16868.	3.8	47
43	How to treat powders for the room temperature aerosol deposition method to avoid porous, low strength ceramic films. Journal of the European Ceramic Society, 2019, 39, 592-600.	5.7	47
44	High Versatility and Stability of Mechanochemically Synthesized Halide Perovskite Powders for Optoelectronic Devices. ACS Applied Materials & amp; Interfaces, 2019, 11, 30259-30268.	8.0	47
45	Integrating nitrogen oxide sensor: A novel concept for measuring low concentrations in the exhaust gas. Sensors and Actuators B: Chemical, 2010, 145, 756-761.	7.8	46
46	Nanosized titania derived from a novel sol–gel process for ammonia gas sensor applications. Sensors and Actuators B: Chemical, 2011, 153, 329-334.	7.8	46
47	Controlled Synthesis of Water-Soluble Conjugated Polyelectrolytes Leading to Excellent Hole Transport Mobility. Chemistry of Materials, 2014, 26, 1992-1998.	6.7	46
48	Investigating solid polymer and ceramic electrolytes for lithium-ion batteries by means of an extended Distribution of Relaxation Times analysis. Electrochimica Acta, 2020, 344, 136060.	5.2	45
49	Human Eukaryotic Initiation Factor EIF2C1 Gene: cDNA Sequence, Genomic Organization, Localization to Chromosomal Bands 1p34–p35, and Expression. Genomics, 1999, 61, 210-218.	2.9	44
50	Conductometric Soot Sensor for Automotive Exhausts: Initial Studies. Sensors, 2010, 10, 1589-1598.	3.8	43
51	Effect of propene, propane, and methane on conversion and oxidation state of three-way catalysts: a microwave cavity perturbation study. Applied Catalysis B: Environmental, 2015, 165, 369-377.	20.2	43
52	Dependence of the Intrinsic Conductivity Minimum of SrTiO3 Ceramics on the Sintering Atmosphere. Journal of the American Ceramic Society, 1995, 78, 2569-2571.	3.8	42
53	Some practical points to consider with respect to thermal conductivity and electrical resistivity of ceramic substrates for high-temperature gas sensors. Sensors and Actuators B: Chemical, 2015, 213, 541-546.	7.8	42
54	Thick-films of garnet-type lithium ion conductor prepared by the Aerosol Deposition Method: The role of morphology and annealing treatment on the ionic conductivity. Journal of Power Sources, 2017, 361, 61-69.	7.8	42

#	Article	IF	CITATIONS
55	Half-Cell Potential Analysis of an Ammonia Sensor with the Electrochemical Cell Au YSZ Au, V2O5-WO3-TiO2. Sensors, 2013, 13, 4760-4780.	3.8	41
56	Catalyst State Observation via the Perturbation of a Microwave Cavity Resonator. Frequenz, 2008, 62, .	0.9	40
57	Monitoring the Ammonia Loading of Zeoliteâ€Based Ammonia SCR Catalysts by a Microwave Method. Chemical Engineering and Technology, 2011, 34, 791-796.	1.5	40
58	Reversible Laserâ€Induced Amplified Spontaneous Emission from Coexisting Tetragonal and Orthorhombic Phases in Hybrid Lead Halide Perovskites. Advanced Optical Materials, 2016, 4, 917-928.	7.3	40
59	A finite element model for mixed potential sensors. Sensors and Actuators B: Chemical, 2019, 287, 476-485.	7.8	40
60	Detection of the ammonia loading of a Cu Chabazite SCR catalyst by a radio frequency-based method. Sensors and Actuators B: Chemical, 2014, 205, 88-93.	7.8	39
61	Ammonia storage studies on H-ZSM-5 zeolites by microwave cavity perturbation: correlation of dielectric properties with ammonia storage. Journal of Sensors and Sensor Systems, 2015, 4, 263-269.	0.9	39
62	Zeolite-based Impedimetric Gas Sensor Device in Low-cost Technology for Hydrocarbon Gas Detection. Sensors, 2008, 8, 7904-7916.	3.8	38
63	Powder aerosol deposition method— novel applications in the field of sensing and energy technology. Functional Materials Letters, 2019, 12, 1930005.	1.2	38
64	Tuning of the electrical conductivity of Sr(Ti,Fe)O3 oxygen sensing films by aerosol co-deposition with Al2O3. Sensors and Actuators B: Chemical, 2016, 230, 427-433.	7.8	37
65	Improvement of the selectivity of the electrochemical conversion of CO2 to hydrocarbons using cupreous electrodes with in-situ oxidation by oxygen. Electrochimica Acta, 2017, 224, 642-648.	5.2	37
66	Materials and applications of polymer films for power capacitors with special respect to nanocomposites. IEEE Transactions on Dielectrics and Electrical Insulation, 2018, 25, 2429-2442.	2.9	37
67	Electron mobility of Sr 1-x La x TiO 3 ceramics between 600 °C and 1300 °C. Applied Physics A: Materials Science and Processing, 1997, 65, 291-294.	2.3	36
68	Sensor for directly determining the exhaust gas recirculation rate—EGR sensor. Sensors and Actuators B: Chemical, 2006, 119, 57-63.	7.8	36
69	Determination of the NOx Loading of an Automotive Lean NOx Trap by Directly Monitoring the Electrical Properties of the Catalyst Material Itself. Sensors, 2011, 11, 8261-8280.	3.8	36
70	ZSM-5 zeolite films on Si substrates grown by in situ seeding and secondary crystal growth and application in an electrochemical hydrocarbon gas sensor. Microporous and Mesoporous Materials, 2008, 111, 530-535.	4.4	35
71	Direct detection of formaldehyde in air by a novel NAD+- and glutathione-independent formaldehyde dehydrogenase-based biosensor. Talanta, 2008, 75, 786-791.	5.5	35
72	What Happens during Thermal Postâ€Treatment of Powder Aerosol Deposited Functional Ceramic Films? Explanations Based on an Experimentâ€Enhanced Literature Survey. Advanced Materials, 2020, 32, e1908104.	21.0	35

#	Article	IF	CITATIONS
73	Thick-film impedance based hydrocarbon detection based on chromium(III) oxide/zeolite interfaces. Sensors and Actuators B: Chemical, 2006, 118, 73-77.	7.8	34
74	In-Operation Monitoring of the Soot Load of Diesel Particulate Filters: Initial Tests. Topics in Catalysis, 2013, 56, 483-488.	2.8	34
75	Ammonia Loading Detection of Zeolite SCR Catalysts using a Radio Frequency based Method. SAE International Journal of Engines, 0, 8, 1126-1135.	0.4	34
76	Recent Developments in the Field of Automotive Exhaust Gas Ammonia Sensing. Sensor Letters, 2008, 6, 821-825.	0.4	34
77	Overview on conductometric solid-state gas dosimeters. Journal of Sensors and Sensor Systems, 2014, 3, 29-46.	0.9	34
78	Aerosol deposition of (Cu,Ti) substituted bismuth vanadate films. Thin Solid Films, 2014, 573, 185-190.	1.8	33
79	Layered Ceramic Phosphors Based on CaAlSiN ₃ :Eu and YAG:Ce for White Lightâ€Emitting Diodes. Journal of the American Ceramic Society, 2016, 99, 211-217.	3.8	33
80	Poisoning of Temperature Independent Resistive Oxygen Sensors by Sulfur Dioxide. Journal of Electroceramics, 2004, 13, 733-738.	2.0	32
81	Zeolite cover layer for selectivity enhancement of p-type semiconducting hydrocarbon sensors. Sensors and Actuators B: Chemical, 2008, 133, 502-508.	7.8	32
82	The effect of Cu and Fe cations on NH3-supported proton transport in DeNOx-SCR zeolite catalysts. Catalysis Science and Technology, 2016, 6, 3362-3366.	4.1	32
83	Solid state mixed-potential sensors as direct conversion sensors for automotive catalysts. Sensors and Actuators B: Chemical, 2018, 255, 3025-3032.	7.8	32
84	Metal Loading Affects the Proton Transport Properties and the Reaction Monitoring Performance of Fe-ZSM-5 and Cu-ZSM-5 in NH ₃ -SCR. Journal of Physical Chemistry C, 2016, 120, 25361-25370.	3.1	31
85	Correlating the Integral Sensing Properties of Zeolites with Molecular Processes by Combining Broadband Impedance and DRIFT Spectroscopy—A New Approach for Bridging the Scales. Sensors, 2015, 15, 28915-28941.	3.8	30
86	Mechanistic Understanding of Cu-CHA Catalyst as Sensor for Direct NH ₃ -SCR Monitoring: The Role of Cu Mobility. ACS Applied Materials & Interfaces, 2019, 11, 8097-8105.	8.0	30
87	Pulsed potential electrochemical CO2 reduction for enhanced stability and catalyst reactivation of copper electrodes. Electrochemistry Communications, 2020, 121, 106861.	4.7	30
88	Direct Thermoelectric Hydrocarbon Gas Sensors Based on \${m SnO}_{2}\$. IEEE Sensors Journal, 2007, 7, 1490-1496.	4.7	29
89	Modeling of hydrocarbon sensors based on p-type semiconducting perovskites. Physical Chemistry Chemical Physics, 2007, 9, 635-642.	2.8	28
90	Miniaturized low temperature co-fired ceramics (LTCC) biosensor for amperometric gas sensing. Sensors and Actuators B: Chemical, 2008, 135, 89-95.	7.8	28

#	Article	IF	CITATIONS
91	Microscopic (Dis)order and Dynamics of Cations in Mixed FA/MA Lead Halide Perovskites. Journal of Physical Chemistry C, 2021, 125, 1742-1753.	3.1	28
92	Analysis of volatile alcohols in apple juices by an electrochemical biosensor measuring in the headspace above the liquid. Sensors and Actuators B: Chemical, 2011, 158, 313-318.	7.8	27
93	Thermoelectric hydrocarbon sensor in thick-film technology for on-board-diagnostics of a diesel oxidation catalyst. Sensors and Actuators B: Chemical, 2015, 214, 234-240.	7.8	27
94	Amperometric Enzymeâ€Based Biosensor for Direct Detection of Formaldehyde in the Gas Phase: Dependence on Electrolyte Composition. Electroanalysis, 2008, 20, 410-417.	2.9	26
95	Electrical In Situ Characterization of Three-Way Catalyst Coatings. Topics in Catalysis, 2009, 52, 1898-1902.	2.8	26
96	Combination of Wirebound and Microwave Measurements for In Situ Characterization of Automotive Three-Way Catalysts. IEEE Sensors Journal, 2011, 11, 434-438.	4.7	26
97	Overview: Status of the Microwave-Based Automotive Catalyst State Diagnosis. Topics in Catalysis, 2013, 56, 358-364.	2.8	26
98	Microwave-Based Catalyst State Diagnosis - State of the Art and Future Perspectives. SAE International Journal of Engines, 2015, 8, 1240-1245.	0.4	26
99	CO2 Selective Potentiometric Sensor in Thick-film Technology. Sensors, 2008, 8, 4774-4785.	3.8	25
100	TWC: Lambda Control and OBD without Lambda Probe - An Initial Approach. , 0, , .		25
101	Porous and non-porous micrometer-sized glass platelets as separators for lithium-ion batteries. Journal of Membrane Science, 2018, 550, 518-525.	8.2	25
102	Thermal Treatment of Aerosol Deposited NiMn2O4 NTC Thermistors for Improved Aging Stability. Sensors, 2018, 18, 3982.	3.8	25
103	Effect of the Heterogeneous Catalytic Activity of Electrodes for Mixed Potential Sensors. Journal of the Electrochemical Society, 2018, 165, B795-B803.	2.9	25
104	The Aerosol Deposition Method: A Modified Aerosol Generation Unit to Improve Coating Quality. Materials, 2018, 11, 1572.	2.9	25
105	Aerosol-deposited BaFe _{0.7} Ta _{0.3} O <s for nitrogen monoxide and temperature-independent oxygen sensing. Journal of Sensors and Sensor Systems, 2014, 3, 223-229.</s 	ub&e	r t;3-Ĵ <
106	Sulfur adsorber for thick-film exhaust gas sensors. Sensors and Actuators B: Chemical, 2003, 93, 36-42.	7.8	24
107	Electrodeposited and Sol-gel Precipitated p-type SrTi1-xFexO3-δSemiconductors for Gas Sensing. Sensors, 2007, 7, 1871-1886.	3.8	24
108	Microwave Cavity Perturbation as a Tool for Laboratory In Situ Measurement of the Oxidation State of Three Way Catalysts. Topics in Catalysis, 2013, 56, 405-409.	2.8	24

#	Article	IF	CITATIONS
109	Influence of Oxygen Partial Pressure during Processing on the Thermoelectric Properties of Aerosol-Deposited CuFeO2. Materials, 2016, 9, 227.	2.9	24
110	Monitoring NH3 storage and conversion in Cu-ZSM-5 and Cu-SAPO-34 catalysts for NH3-SCR by simultaneous impedance and DRIFT spectroscopy. Sensors and Actuators B: Chemical, 2016, 236, 1075-1082.	7.8	24
111	Effect of electrodes and zeolite cover layer on hydrocarbon sensing with p-type perovskite SrTi0.8Fe0.2O3-δthick and thin films. Journal of Materials Science, 2006, 41, 5828-5835.	3.7	23
112	Response kinetics of temperature-independent resistive oxygen sensor formulations: a comparative study. Sensors and Actuators B: Chemical, 2006, 113, 112-119.	7.8	23
113	Direct monitoring of organic vapours with amperometric enzyme gas sensors. Biosensors and Bioelectronics, 2010, 25, 1521-1525.	10.1	23
114	Microwave-Based Oxidation State and Soot Loading Determination on Gasoline Particulate Filters with Three-Way Catalyst Coating for Homogenously Operated Gasoline Engines. Sensors, 2015, 15, 21971-21988.	3.8	23
115	A microwave-based method to monitor the ammonia loading of a vanadia-based SCR catalyst. Applied Catalysis B: Environmental, 2015, 165, 36-42.	20.2	23
116	Self-heated HTCC-based ceramic disc for mixed potential sensors and for direct conversion sensors for automotive catalysts. Sensors and Actuators B: Chemical, 2017, 248, 793-802.	7.8	23
117	High-Temperature Electrical Insulation Behavior of Alumina Films Prepared at Room Temperature by Aerosol Deposition and Influence of Annealing Process and Powder Impurities. Journal of Thermal Spray Technology, 2018, 27, 870-879.	3.1	23
118	Synthesis, Structure, and Electric Conductivity of Ferrous Tainiolite and Its Oxidative Conversion into Coarse-Grained Swellable Smectite. Chemistry of Materials, 2007, 19, 5377-5387.	6.7	22
119	α-Iron oxide: An intrinsically semiconducting oxide material for direct thermoelectric oxygen sensors. Sensors and Actuators B: Chemical, 2010, 145, 685-690.	7.8	22
120	Novel tube-type LTCC transducers with buried heaters and inner interdigitated electrodes as a platform for gas sensing at various high temperatures. Sensors and Actuators B: Chemical, 2013, 189, 80-88.	7.8	22
121	Compact Layers of Hybrid Halide Perovskites Fabricated via the Aerosol Deposition Process—Uncoupling Material Synthesis and Layer Formation. Materials, 2016, 9, 277.	2.9	22
122	Effects of H2O, CO2, CO, and Flow Rates on the RF-Based Monitoring of Three-Way Catalysts. Sensor Letters, 2011, 9, 316-320.	0.4	22
123	Improvement of the sensitivity of a conductometric soot sensor by adding a conductive cover layer. Journal of Sensors and Sensor Systems, 2013, 2, 95-102.	0.9	22
124	Temperature-modulated direct thermoelectric gas sensors: thermal modeling and results for fast hydrocarbon sensors. Measurement Science and Technology, 2009, 20, 065205.	2.6	21
125	Miniaturized ceramic differential scanning calorimeter with integrated oven and crucible in LTCC technology. Sensors and Actuators A: Physical, 2011, 172, 21-26.	4.1	21
126	In operando Detection of Three-Way Catalyst Aging by a Microwave-Based Method: Initial Studies. Applied Sciences (Switzerland), 2015, 5, 174-186.	2.5	21

#	Article	IF	CITATIONS
127	Sensing catalytic conversion: Simultaneous DRIFT and impedance spectroscopy for in situ monitoring of NH3–SCR on zeolites. Sensors and Actuators B: Chemical, 2016, 224, 492-499.	7.8	21
128	Magnetization in insulating phases of Ti4+-doped SrFeO3â~δ. Journal of Applied Physics, 2006, 99, 08S904.	2.5	20
129	Gas Diffusion Electrodes for Use in an Amperometric Enzyme Biosensor. Electroanalysis, 2008, 20, 2279-2286.	2.9	20
130	Amperometric Enzyme-based Gas Sensor for Formaldehyde: Impact of Possible Interferences. Sensors, 2008, 8, 1351-1365.	3.8	20
131	Thick-film solid electrolyte oxygen sensors using the direct ionic thermoelectric effect. Sensors and Actuators B: Chemical, 2009, 136, 530-535.	7.8	20
132	In situ Monitoring of Coke Deposits during Coking and Regeneration of Solid Catalysts by Electrical Impedanceâ€based Sensors. Chemical Engineering and Technology, 2010, 33, 103-112.	1.5	20
133	Planar potentiometric SO2 gas sensor for high temperatures using NASICON electrolyte combined with V2O5/WO3/TiO2 + Au or Pt electrode. Journal of the Ceramic Society of Japan, 2011, 119, 687-691.	1.1	20
134	Vanadia doped tungsten–titania SCR catalysts as functional materials for exhaust gas sensor applications. Sensors and Actuators B: Chemical, 2011, 155, 199-205.	7.8	20
135	Gas sensing of ruthenium implanted tungsten oxide thin films. Thin Solid Films, 2014, 558, 416-422.	1.8	20
136	Aerosol Codeposition of Ceramics: Mixtures of Bi ₂ O ₃ –TiO ₂ and Bi ₂ O ₃ –V ₂ O ₅ . Journal of the American Ceramic Society, 2015, 98, 717-723.	3.8	20
137	Mechanical Coating of Zinc Particles with Bi2O3-Li2O-ZnO Glasses as Anode Material for Rechargeable Zinc-Based Batteries. Batteries, 2018, 4, 12.	4.5	20
138	The influence of nanoparticles and their functionalization on the dielectric properties of biaxially oriented polypropylene for power capacitors. IEEE Transactions on Dielectrics and Electrical Insulation, 2020, 27, 468-475.	2.9	20
139	Four-Wire Impedance Spectroscopy on Planar Zeolite/Chromium Oxide Based Hydrocarbon Gas Sensors. Sensors, 2007, 7, 2681-2692.	3.8	19
140	Processing issues related to the bi-dimensional ionic conductivity of BIMEVOX ceramics. Journal of Materials Science, 2011, 46, 5447-5453.	3.7	19
141	A mixed potential based sensor that measures directly catalyst conversion—A novel approach for catalyst on-board diagnostics. Sensors and Actuators B: Chemical, 2015, 217, 158-164.	7.8	19
142	Microwave Cavity Perturbation Studies on H-form and Cu Ion-Exchanged SCR Catalyst Materials: Correlation of Ammonia Storage and Dielectric Properties. Topics in Catalysis, 2017, 60, 243-249.	2.8	19
143	Detection of water droplets on exhaust gas sensors. Sensors and Actuators B: Chemical, 2010, 148, 624-629.	7.8	18
144	The Effect of the Thickness of the Sensitive Layer on the Performance of the Accumulating NOx Sensor. Sensors, 2012, 12, 12329-12346.	3.8	18

#	Article	IF	CITATIONS
145	Determining the total amount of NOx in a gas stream – Advances in the accumulating gas sensor principle. Sensors and Actuators B: Chemical, 2012, 175, 157-162.	7.8	18
146	Radio-Frequency-Based Urea Dosing Control for Diesel Engines with Ammonia SCR Catalysts. SAE International Journal of Engines, 0, 10, 1638-1645.	0.4	18
147	On the influence of the NO equilibrium reaction on mixed potential sensor signals: A comparison between FE modelling and experimental data. Sensors and Actuators B: Chemical, 2019, 296, 126627.	7.8	18
148	Solid Electrolyte Hydrocarbon Gas Sensor Using Zeolite as the Sensitive Phase. Electrochemical and Solid-State Letters, 2006, 9, H31.	2.2	17
149	Selectivity enhancement of p-type semiconducting hydrocarbon sensors—The use of sol-precipitated nano-powders. Sensors and Actuators B: Chemical, 2008, 130, 470-476.	7.8	17
150	Pulsed polarization of platinum electrodes on YSZ. Solid State Ionics, 2012, 225, 371-375.	2.7	17
151	BaFe1-xTaxO3-δ– A material for temperature independent resistive oxygen sensors. Sensors and Actuators B: Chemical, 2014, 190, 208-213.	7.8	17
152	Thermal, dielectric, and mechanical properties of hâ€BNâ€filled PTFE composites. Journal of Applied Polymer Science, 2018, 135, 46859.	2.6	17
153	Flexible, Heat-Resistant, and Flame-Retardant Glass Fiber Nonwoven/Glass Platelet Composite Separator for Lithium-Ion Batteries. Energies, 2018, 11, 999.	3.1	17
154	Morphology dependence of thermopower and conductance in semiconducting oxides with space charge regions. Solid State Ionics, 2008, 179, 2299-2307.	2.7	16
155	Sensor for Directly Determining the State of a NOx Storage Catalyst. , 2008, , .		16
156	Perovskite-type proton conductor for novel direct ionic thermoelectric hydrogen sensor. Solid State Ionics, 2011, 192, 101-104.	2.7	16
157	Planar Zeolite Film-Based Potentiometric Gas Sensors Manufactured by a Combined Thick-Film and Electroplating Technique. Sensors, 2011, 11, 7736-7748.	3.8	16
158	Capacitive soot sensor for diesel exhausts. Sensors and Actuators B: Chemical, 2016, 236, 1020-1027.	7.8	16
159	Comparative Study of Different Methods for Soot Sensing and Filter Monitoring in Diesel Exhausts. Sensors, 2017, 17, 400.	3.8	16
160	Influence of the calcination procedure on the thermoelectric properties of calcium cobaltite Ca3Co4O9. Journal of Electroceramics, 2018, 40, 225-234.	2.0	16
161	Integrating NOx Sensor for Automotive Exhausts—A Novel Concept. Sensor Letters, 2011, 9, 311-315.	0.4	16
162	Combined resistive and thermoelectric oxygen sensor with almost temperature-independent characteristics. Journal of Sensors and Sensor Systems, 2018, 7, 289-297.	0.9	16

#	Article	lF	CITATIONS
163	Impedance spectroscopy of Na+ conducting zeolite ZSM-5. Solid State Ionics, 2006, 177, 2321-2323.	2.7	15
164	Cuprate-ferrate compositions for temperature independent resistive oxygen sensors. Journal of Electroceramics, 2006, 16, 179-186.	2.0	15
165	Resistive NOx dosimeter to detect very low NOx concentrations—Proof-of-principle and comparison with classical sensing devices. Sensors and Actuators B: Chemical, 2017, 248, 848-855.	7.8	15
166	Influence of pressure assisted sintering and reaction sintering on microstructure and thermoelectric properties of bi-doped and undoped calcium cobaltite. Journal of Applied Physics, 2019, 126, .	2.5	15
167	Novel Operation Strategy to Obtain a Fast Gas Sensor for Continuous ppb-Level NO2 Detection at Room Temperature Using ZnO—A Concept Study with Experimental Proof. Sensors, 2019, 19, 4104.	3.8	15
168	Determination of the Dielectric Properties of Storage Materials for Exhaust Gas Aftertreatment Using the Microwave Cavity Perturbation Method. Sensors, 2020, 20, 6024.	3.8	15
169	Magnetic and ferroelectric properties of Fe doped SrTiO _{3-δ} films. Journal of Physics: Conference Series, 2010, 200, 092010.	0.4	14
170	Effect of substrate hardness and surface roughness on the film formation of aerosol-deposited ceramic films. Functional Materials Letters, 2017, 10, 1750045.	1.2	14
171	Pulsed Polarization-Based NOx Sensors of YSZ Films Produced by the Aerosol Deposition Method and by Screen-Printing. Sensors, 2017, 17, 1715.	3.8	14
172	Powder Pre-Treatment for Aerosol Deposition of Tin Dioxide Coatings for Gas Sensors. Materials, 2018, 11, 1342.	2.9	14
173	Impact of Pressure and Temperature on the Compaction Dynamics and Layer Properties of Powder-Pressed Methylammonium Lead Halide Thick Films. ACS Applied Electronic Materials, 2020, 2, 2619-2628.	4.3	14
174	Powder Aerosol Deposition as a Method to Produce Garnetâ€Type Solid Ceramic Electrolytes: A Study on Electrochemical Film Properties and Industrial Applications. Energy Technology, 2021, 9, 2100211.	3.8	14
175	Electrical Conductivity of Halide Perovskites Follows Expectations from Classical Defect Chemistry. European Journal of Inorganic Chemistry, 2021, 2021, 2882-2889.	2.0	14
176	HC-sensor for exhaust gases based on semiconducting doped SrTiO3 for On-Board Diagnosis. Sensors and Actuators B: Chemical, 2006, 114, 861-868.	7.8	13
177	Method for reliable detection of different exhaust gas components by pulsed discharge measurements using standard zirconia based sensors. Procedia Chemistry, 2009, 1, 585-588.	0.7	13
178	Direct detection of coke deposits on fixed bed catalysts by electrical sensors. Sensors and Actuators B: Chemical, 2010, 144, 437-442.	7.8	13
179	Mikrowellengestützte Aufkläung elektrochemischer Vorgäge in Katalysatoren und verwandten Systemen. TM Technisches Messen, 2010, 77, 419-427.	0.7	13
180	Conductometric Sensor for Soot Mass Flow Detection in Exhausts of Internal Combustion Engines. Sensors, 2015, 15, 28796-28806.	3.8	13

#	Article	IF	CITATIONS
181	Superconducting Properties of Thick Films on Hastelloy Prepared by the Aerosol Deposition Method With Ex Situ MgB2 Powder. IEEE Transactions on Applied Superconductivity, 2017, 27, 1-4.	1.7	13
182	Effect of Oxygen Partial Pressure on the Phase Stability of Copper–Iron Delafossites at Elevated Temperatures. Materials, 2018, 11, 1888.	2.9	13
183	Conductometric Soot Sensors: Internally Caused Thermophoresis as an Important Undesired Side Effect. Sensors, 2018, 18, 3531.	3.8	13
184	In- and through-plane conductivity of 8YSZ films produced at room temperature by aerosol deposition. Journal of Materials Science, 2019, 54, 13619-13634.	3.7	13
185	Oxidation State and Dielectric Properties of Ceria-Based Catalysts by Complementary Microwave Cavity Perturbation and X-Ray Absorption Spectroscopy Measurements. Topics in Catalysis, 2019, 62, 227-236.	2.8	13
186	Potentiometric hydrocarbon gas sensing characteristics of sodium ion conducting zeolite ZSM-5. Sensors and Actuators B: Chemical, 2008, 130, 546-550.	7.8	12
187	Anisotropy and thermal stability of hot-forged BICUTIVOX oxygen ion conducting ceramics. Journal of the European Ceramic Society, 2014, 34, 943-951.	5.7	12
188	SI-Engine Control With Microwave-Assisted Direct Observation of Oxygen Storage Level in Three-Way Catalysts. IEEE Transactions on Control Systems Technology, 2014, 22, 2346-2353.	5.2	12
189	Annealing of Gadolinium-Doped Ceria (GDC) Films Produced by the Aerosol Deposition Method. Materials, 2018, 11, 2072.	2.9	12
190	Catalyst State Diagnosis of Three-Way Catalytic Converters Using Different Resonance Parameters—A Microwave Cavity Perturbation Study. Sensors, 2019, 19, 3559.	3.8	12
191	A new potentiometric NO sensor based on a NO+ cation conducting ceramic membrane. Sensors and Actuators B: Chemical, 2001, 77, 287-292.	7.8	11
192	Ceramic Alumina Substrates for High-temperature Gas Sensors – Implications for Applicability. Procedia Engineering, 2014, 87, 1505-1508.	1.2	11
193	Screen-printable Type S Thermocouple for Thick-film Technology. Procedia Engineering, 2015, 120, 828-831.	1.2	11
194	Influencing Parameters on the Microwave-Based Soot Load Determination of Diesel Particulate Filters. Topics in Catalysis, 2017, 60, 374-380.	2.8	11
195	Novel Method for NTC Thermistor Production by Aerosol Co-Deposition and Combined Sintering. Sensors, 2019, 19, 1632.	3.8	11
196	Selectivity improvement towards hydrogen and oxygen of solid electrolyte sensors by dynamic electrochemical methods. Sensors and Actuators B: Chemical, 2019, 290, 53-58.	7.8	11
197	Manufacturing Dense Thick Films of Lunar Regolith Simulant EAC-1 at Room Temperature. Materials, 2019, 12, 487.	2.9	11
198	Radio-Frequency-Based NH3-Selective Catalytic Reduction Catalyst Control: Studies on Temperature Dependency and Humidity Influences. Sensors, 2017, 17, 1615.	3.8	10

#	Article	IF	CITATIONS
199	Laserâ€Annealing of Thermoelectric CuFe 0.98 Sn 0.02 O 2 Films Produced by Powder Aerosol Deposition Method. Advanced Materials Interfaces, 2020, 7, 2001114.	3.7	10
200	Influence of Humidity and Different Gases on a Resistive Room Temperature NO ₂ Gas Dosimeter Based on Al-Doped ZnO for ppb-Concentration Detection. Journal of the Electrochemical Society, 2020, 167, 167516.	2.9	10
201	SINGLE CRYSTAL GROWTH AND TEXTURING OF LEAD-BASED PIEZOELECTRIC CERAMICS VIA TEMPLATED GRAIN GROWTH PROCESS. Functional Materials Letters, 2008, 01, 127-132.	1.2	9
202	Direct detection of coking and regeneration of single particles and fixed bed reactors by electrical sensors. Applied Catalysis A: General, 2010, 382, 254-262.	4.3	9
203	Amperometric enzyme electrodes for the determination of volatile alcohols in the headspace above fruit and vegetable juices. Mikrochimica Acta, 2012, 179, 115-121.	5.0	9
204	The effect of SO2 on the sensitive layer of a NOx dosimeter. Sensors and Actuators B: Chemical, 2013, 187, 153-161.	7.8	9
205	In situ detection of coke deposits on fixed-bed catalysts by a radio frequency-based method. Sensors and Actuators B: Chemical, 2013, 181, 681-689.	7.8	9
206	Review on Radio Frequency Based Monitoring of SCR and Three Way Catalysts. Topics in Catalysis, 2016, 59, 961-969.	2.8	9
207	Radio Frequency-Based Determination of the Oxygen and the NOx Storage Level of NOx Storage Catalysts. Topics in Catalysis, 2019, 62, 157-163.	2.8	9
208	Linking the Electrical Conductivity and Non-Stoichiometry of Thin Film Ce1â^'xZrxO2â^'δ by a Resonant Nanobalance Approach. Materials, 2021, 14, 748.	2.9	9
209	Investigation of the Powder Aerosol Deposition Method Using Shadowgraph Imaging. Materials, 2021, 14, 2502.	2.9	9
210	Geometrical, electrical and stability properties of thickâ€film and LTCC microcapacitors. Microelectronics International, 2008, 25, 37-41.	0.6	8
211	Integrated impedance based hydroâ€carbon gas sensors with Naâ€zeolite/Cr ₂ O ₃ thinâ€film interfaces: From physical modeling to devices. Physica Status Solidi (A) Applications and Materials Science, 2011, 208, 404-415.	1.8	8
212	The electrical properties of NOx-storing carbonates during NOx exposure. Solid State Ionics, 2012, 225, 317-323.	2.7	8
213	Electrical conductivity study of NOx trap materials BaCO3 and K2CO3/La-Al2O3 during NOx exposure. Sensors and Actuators B: Chemical, 2013, 187, 461-470.	7.8	8
214	Dosimeter-Type NOx Sensing Properties of KMnO4 and Its Electrical Conductivity during Temperature Programmed Desorption. Sensors, 2013, 13, 4428-4449.	3.8	8
215	Detection of NO by pulsed polarization of Pt I YSZ. Solid State Ionics, 2014, 262, 288-291.	2.7	8
216	Determination of the Soot Mass by Conductometric Soot Sensors. Procedia Engineering, 2014, 87, 244-247.	1.2	8

#	Article	IF	CITATIONS
217	In situ monitoring of DeNO x -SCR on zeolite catalysts by means of simultaneous impedance and DRIFT spectroscopy. Procedia Engineering, 2015, 120, 257-260.	1.2	8
218	Miniaturized ceramic DSC device with strain gauge-based mass detection—First steps to realize a fully integrated DSC/TGA device. Sensors and Actuators A: Physical, 2016, 241, 145-151.	4.1	8
219	Analysis of the characteristics of thick-film NTC thermistor devices manufactured by screen-printing and firing technique and by room temperature aerosol deposition method (ADM). Functional Materials Letters, 2017, 10, 1750073.	1.2	8
220	Radio-Frequency-Controlled Urea Dosing for NH3-SCR Catalysts: NH3 Storage Influence to Catalyst Performance under Transient Conditions. Sensors, 2017, 17, 2746.	3.8	8
221	On the defect chemistry of BaFe0.89Al0.01Ta0.1O3â€; a material for temperature independent resistive and thermoelectric oxygen sensors. Solid State Ionics, 2018, 316, 1-8.	2.7	8
222	Improved Discharge Capacity of Zinc Particles by Applying Bismuth-Doped Silica Coating for Zinc-Based Batteries. Batteries, 2019, 5, 32.	4.5	8
223	Comparison of the electrical conductivity of bulk and film Ce1–xZrxO2â€"î´ in oxygen-depleted atmospheres at high temperatures. Journal of Materials Science, 2021, 56, 17191-17204.	3.7	8
224	An Initial Physics-Based Model for the Impedance Spectrum of a Hydrocarbon Sensor with a Zeolite/Cr ₂ O ₃ Interface. Sensor Letters, 2008, 6, 1019-1022.	0.4	8
225	Ion onducting Probes for Low Temperature Plasmas. Contributions To Plasma Physics, 2008, 48, 473-479.	1.1	7
226	Calorimetric sensitivity and thermal resolution of a novel miniaturized ceramic DSC chip in LTCC technology. Thermochimica Acta, 2012, 543, 142-149.	2.7	7
227	Automotive Catalyst State Diagnosis Using Microwaves. Oil and Gas Science and Technology, 2015, 70, 55-65.	1.4	7
228	Influence of high temperature annealing on the dielectric properties of alumina films prepared by the aerosol deposition method. Functional Materials Letters, 2018, 11, 1850022.	1.2	7
229	First steps to develop a sensor for a Tian–Calvet calorimeter with increased sensitivity. Journal of Sensors and Sensor Systems, 2016, 5, 205-212.	0.9	7
230	Platform to develop exhaust gas sensors manufactured by glass-solder-supported joining of sintered yttria-stabilized zirconia. Journal of Sensors and Sensor Systems, 2016, 5, 25-32.	0.9	7
231	Thin-film chemical expansion of ceria based solid solutions: laser vibrometry study. Zeitschrift Fur Physikalische Chemie, 2022, 236, 1013-1053.	2.8	7
232	On the inverse problem associated with the observation of electrochemical processes by the RF cavity perturbation method. , 2009, , .		6
233	Investigation of the short-time high-current behavior of vias manufactured in hybrid thick-film technology. Microelectronics Reliability, 2011, 51, 1257-1263.	1.7	6
234	Failure of electrical vias manufactured in thick-film technology when loaded with short high current pulses. Microelectronics Reliability, 2016, 56, 121-128.	1.7	6

#	Article	IF	CITATIONS
235	Sensor Tool for Fast Catalyst Material Characterization. Topics in Catalysis, 2017, 60, 312-317.	2.8	6
236	High-yield synthesis of ZnO nanoparticles homogeneously coated on exfoliated graphite and simplified method to determine the surface coverage. Surface and Coatings Technology, 2017, 325, 445-453.	4.8	6
237	Towards an Electrochemical Immunosensor System with Temperature Control for Cytokine Detection. Sensors, 2018, 18, 1309.	3.8	6
238	Simulation of a NOx Sensor for Model-Based Control of Exhaust Aftertreatment Systems. Topics in Catalysis, 2019, 62, 150-156.	2.8	6
239	Modelling the Influence of Different Soot Types on the Radio-Frequency-Based Load Detection of Gasoline Particulate Filters. Sensors, 2020, 20, 2659.	3.8	6
240	Planar Zeolite-Based Potentiometric Gas Sensors. Sensor Letters, 2011, 9, 110-113.	0.4	6
241	Is it possible to detect in situ the sulfur loading of a fixed bed catalysts with a sensor?. Journal of Sensors and Sensor Systems, 2015, 4, 143-149.	0.9	6
242	Simulation of a thermoelectric gas sensor that determines hydrocarbon concentrations in exhausts and the light-off temperature of catalyst materials. Journal of Sensors and Sensor Systems, 2017, 6, 395-405.	0.9	6
243	A pathway to eliminate the gas flow dependency of a hydrocarbon sensor for automotive exhaust applications. Journal of Sensors and Sensor Systems, 2018, 7, 79-84.	0.9	6
244	Novel radio-frequency-based gas sensor withÂintegratedÂheater. Journal of Sensors and Sensor Systems, 2019, 8, 49-56.	0.9	6
245	Posttreatment of powder aerosol deposited oxide ceramic films by high power LED. International Journal of Applied Ceramic Technology, 2022, 19, 1540-1553.	2.1	6
246	Modern diagnostic methods in the Ewing's sarcoma family: Six patients with histologic soft tissue tumors*. Molecular Diagnosis and Therapy, 1997, 2, 15-22.	1.1	5
247	Platform for a Hydrocarbon Exhaust Gas Sensor Utilizing a Pumping Cell and a Conductometric Sensor. Sensors, 2009, 9, 7498-7508.	3.8	5
248	Single crystal growth in PMN-PT and PMN-PZT. Journal of Materials Science, 2009, 44, 1757-1763.	3.7	5
249	Initial tests to detect quantitatively the coke loading of reforming catalysts by a contactless microwave method. Chemical Engineering and Processing: Process Intensification, 2011, 50, 729-731.	3.6	5
250	Planar platform for temperature dependent four-wire impedance spectroscopy—A novel tool to characterize functional materials. Sensors and Actuators B: Chemical, 2013, 187, 174-183.	7.8	5
251	Semiconducting direct thermoelectric gas sensors. , 2013, , 261-296.		5
252	Optimization of thermoelectric properties of metalâ€oxideâ€based polymer composites. Journal of Applied Polymer Science, 2014, 131, .	2.6	5

#	Article	IF	CITATIONS
253	Electrical conductivity relaxation measurements: Application of low thermal mass heater stick. Solid State Ionics, 2014, 262, 914-917.	2.7	5
254	Detection of NO by Pulsed Polarization Technique Using Pt Interdigital Electrodes on Yttria-stabilized Zirconia. Procedia Engineering, 2014, 87, 620-623.	1.2	5
255	Capacitive Soot Sensor. Procedia Engineering, 2015, 120, 241-244.	1.2	5
256	Radio Frequencyâ€Based In Situ Determination of the Mass Loss of Supported Ionic Liquids. Chemical Engineering and Technology, 2017, 40, 1660-1665.	1.5	5
257	Influence of pressure and dwell time on pressureâ€assisted sintering of calcium cobaltite. Journal of the American Ceramic Society, 2021, 104, 917-927.	3.8	5
258	Suppressed ion migration in powder-based perovskite thick films using an ionic liquid. Journal of Materials Chemistry C, 2021, 9, 11827-11837.	5.5	5
259	<l>P</l> -Type Semiconducting Perovskite Sensors for Reducing Gases—Model Description. Sensor Letters, 2008, 6, 808-811.	0.4	5
260	Multi-gas sensor to detect simultaneously nitrogen oxides and oxygen. Journal of Sensors and Sensor Systems, 2020, 9, 327-335.	0.9	5
261	INFLUENCE OF SINTERING CONDITIONS ON DOPED PZT CERAMICS FOR BASE-METAL ELECTRODE MULTILAYER ACTUATORS. Functional Materials Letters, 2012, 05, 1250022.	1.2	4
262	Novel Tube-Type LTCC Transducers with Buried Heaters and Inner Electrodes for High-Temperatures Gas Sensors. Procedia Engineering, 2012, 47, 60-63.	1.2	4
263	NO Detection by Pulsed Polarization of Lambda Probes–Influence of the Reference Atmosphere. Sensors, 2013, 13, 16051-16064.	3.8	4
264	Undoped and doped poly(tetraphenylbenzidine) as sensitive material for an impedimetric nitrogen dioxide gas dosimeter. Applied Physics Letters, 2014, 105, 133301.	3.3	4
265	Development and Application of a Fast Solid-state Potentiometric CO2-sensor in Thick-film Technology. Procedia Engineering, 2014, 87, 1031-1034.	1.2	4
266	Investigations on the crystal growth mechanism of one-pot-synthesized Al-doped ZnO and its UV-enhanced room temperature NO2 gas sensing characteristics. Functional Materials Letters, 2018, 11, 1850087.	1.2	4
267	Sodium Borosilicate Glass Separators as an Electrolyte Additive Donor for Improving the Electrochemical Performance of Lithium-Ion Batteries. Journal of the Electrochemical Society, 2019, 166, A3416-A3424.	2.9	4
268	Influence of polarization time and polarization current of Pt YSZ-based NO sensors utilizing the pulsed polarization when applying constant charge. Sensors and Actuators B: Chemical, 2019, 290, 28-33.	7.8	4
269	A Synthetic Ash-Loading Method for Gasoline Particulate Filters with Active Oil Injection. SAE International Journal of Engines, 0, 14, 493-505.	0.4	4
270	Making powder aerosol deposition accessible for small amounts: A novel and modular approach to produce dense ceramic films. International Journal of Applied Ceramic Technology, 2021, 18, 2178.	2.1	4

#	Article	IF	CITATIONS
271	Mixing Rules for an Exact Determination of the Dielectric Properties of Engine Soot Using the Microwave Cavity Perturbation Method and Its Application in Gasoline Particulate Filters. Sensors, 2022, 22, 3311.	3.8	4
272	Zeolithe zur Ammoniakdetektion in Abgasen. Zeitschrift Fur Anorganische Und Allgemeine Chemie, 2008, 634, 2077-2077.	1.2	3
273	Laser processing of materials for MCM-C applications. , 2008, , .		3
274	Accumulating gas sensor principle – how to come from concentration integration to real amount measurements. Procedia Engineering, 2011, 25, 1109-1112.	1.2	3
275	Locally resolved in-situ detection of the soot loading in diesel particulate filters. , 2011, , .		3
276	Effect of a porous Pt/alumina cover layer for V ₂ O ₅ /WO ₃ /TiO ₂ resistive SO ₂ sensing materials. Journal of the Ceramic Society of Japan, 2013, 121, 734-737.	1.1	3
277	Particulate Filter Substrates with SCR-Functionality Manufactured by Co-extrusion of Ceramic Substrate and SCR Active Material. Topics in Catalysis, 2017, 60, 204-208.	2.8	3
278	Ultrasound-assisted one-pot syntheses of ZnO nanoparticles that are homogeneously adsorbed on exfoliated graphite and a simplified method to determine the graphite layer thickness in such composites. Journal of Materials Science, 2018, 53, 6586-6601.	3.7	3
279	Radio frequency- and impedance-based sensing of ionic liquids supported on porous carriers and their limitations. Sensors and Actuators B: Chemical, 2018, 273, 1564-1571.	7.8	3
280	Influence of ambient conditions on electrical partial discharge resistance of epoxy anhydride based polymers using IEC 60343 method. IEEE Transactions on Dielectrics and Electrical Insulation, 2019, 26, 1463-1470.	2.9	3
281	Investigation of the <i>in situ</i> calcination of aerosol co-deposited NiO-Mn ₂ O ₃ films. Functional Materials Letters, 2019, 12, 1950039.	1.2	3
282	Powder Treatment for Increased Thickness of Iron Coatings Produced by the Powder Aerosol Deposition Method and Formation of Iron–Alumina Multilayer Structures. Journal of Thermal Spray Technology, 2021, 30, 480-487.	3.1	3
283	Novel, low-cost device to simultaneously measure the electrical conductivity and the Hall coefficient from room temperature up to 600 °C. Journal of Sensors and Sensor Systems, 2021, 10, 71-81.	0.9	3
284	Discontinuous Powder Aerosol Deposition: An Approach to Prepare Films Using Smallest Powder Quantities. Coatings, 2021, 11, 844.	2.6	3
285	Laser forming of LTCC Ceramics for Hot-Plate Gas Sensors. Journal of Microelectronics and Electronic Packaging, 2005, 2, 14-18.	0.7	3
286	Influence of operation temperature variations on NO measurements in low concentrations when applying the pulsed polarization technique to thimble-type lambda probes. Journal of Sensors and Sensor Systems, 2015, 4, 321-329.	0.9	3
287	Analysis of defect chemistry and microstructural effects of non-stoichiometric ceria by the high-temperature microwave cavity perturbation method. Journal of the European Ceramic Society, 2022, 42, 499-511.	5.7	3
288	Contributions of Pulsed Operation Along with Proper Choice of the Substrate for Stabilizing the Catalyst Performance in Electrochemical Reduction of CO ₂ Toward Ethylene in Gas Diffusion Electrode Based Flow Cell Reactors. Energy Technology, 2022, 10, .	3.8	3

#	Article	IF	CITATIONS
289	Temperature-dependent dielectric anomalies in powder aerosol deposited ferroelectric ceramic films. Journal of Materiomics, 2022, 8, 1239-1250.	5.7	3
290	Thick and thin film p-type conducting perovskite hydrocarbon sensors - a comparative study. , 0, , .		2
291	Amperometric measurements with a nitrosyl cation conducting ceramic membrane. Physical Chemistry Chemical Physics, 2003, 5, 5199-5202.	2.8	2
292	An investigation of thick-film materials for temperature and pressure sensors on self-constrained LTCC substrates. , 2008, , .		2
293	Investigation of Oxygen Transport Paths in Geometrically Defined Thick-Film Composite Pt Electrodes on YSZ. Journal of the Electrochemical Society, 2016, 163, F877-F884.	2.9	2
294	Sensitivity Improvement of Thermoelectric Hydrocarbon Sensors: Combination of Glass-Ceramic Tapes and Alumina Substrates. Proceedings (mdpi), 2017, 1, 403.	0.2	2
295	Exhaust Gas Analysis of Firewood Combustion Processes: Application of a Robust Thermoelectric Gas Sensor. Proceedings (mdpi), 2017, 1, 457.	0.2	2
296	High-Yield Preparation of ZnO Nanoparticles on Exfoliated Graphite as Anode Material for Lithium Ion Batteries and the Effect of Particle Size as well as of Conductivity on the Electrochemical Performance of Such Composites. Batteries, 2018, 4, 24.	4.5	2
297	Dielectric properties and temperature dependency of automotive catalyst coatings and substrate materials: Experimental results, influences and approximation approach. Functional Materials Letters, 2019, 12, 1950024.	1.2	2
298	Modelling Both the NH3 Storage on Automotive SCR Catalysts and the Radio-Frequency-Based Response. Topics in Catalysis, 2019, 62, 172-178.	2.8	2
299	Characterization of the sensitive material for a resistive NOx gas dosimeter by DRIFT spectroscopy. Sensors and Actuators B: Chemical, 2020, 320, 128568.	7.8	2
300	Electrical conductivity determination of semiconductors by utilizing photography, finite element simulation and resistance measurement. Journal of Materials Science, 2021, 56, 10449-10457.	3.7	2
301	Monitoring of Electrochemical Processes in Catalysts by Microwave Methods. , 2011, , 119-132.		2
302	Automotive Exhaust Gas Sensor Based on an Electrochemical Cell Combined with a Resistive Gas Sensor. Sensor Letters, 2008, 6, 803-807.	0.4	2
303	Potentiometric CO ₂ Gas Sensor Based on Zeolites. Sensor Letters, 2011, 9, 902-906.	0.4	2
304	Hochfrequenzsensorik zur direkten Beladungserkennung von Benzinpartikelfiltern. , 2020, , 185-208.		2
305	Cyclic and square-wave voltammetry for selective simultaneous NO and O ₂ gas detection by means of solid electrolyte sensors. Journal of Sensors and Sensor Systems, 2020, 9, 355-362.	0.9	2
306	Glassâ€ceramic composites as insulation material for thermoelectric oxide multilayer generators. Journal of the American Ceramic Society, 2022, 105, 2140-2149.	3.8	2

#	Article	IF	CITATIONS
307	From Thermoelectric Powder Directly to Thermoelectric Generators: Flexible Bi ₂ Te ₃ Films on Polymer Sheets Prepared by the Powder Aerosol Deposition Method at Room Temperature. Energy Technology, 2022, 10, .	3.8	2
308	High-load resistors of doped titanate ceramics showing PTCR behavior in the entire temperature range of operation. Journal of the European Ceramic Society, 1999, 19, 759-763.	5.7	1
309	Thermoelectric Hydrocarbon Sensor in Thick-film Technology for On-Board-Diagnostics of a Diesel Oxidation Catalyst. Procedia Engineering, 2014, 87, 616-619.	1.2	1
310	Why does the Conductivity of a Nickel Catalyst Increase during Sulfidation? An Exemplary Study Using an In Operando Sensor Device. Sensors, 2015, 15, 27021-27034.	3.8	1
311	Oxygen transport paths in screen-printed Pt-Al2O3 composite model electrodes on YSZ. Solid State Ionics, 2018, 316, 53-58.	2.7	1
312	Operando Determination of the Thermal Decomposition of Supported Ionic Liquids by a Radio-Frequency-Based Method. ACS Omega, 2019, 4, 3351-3360.	3.5	1
313	Oxygen partial pressure dependency of the electrical conductivity of aerosol deposited alumina films between 650â€ ⁻ °C and 900â€ ⁻ °C. Materials Letters, 2019, 245, 208-210.	2.6	1
314	Determination of water loading of supported ionic liquids by microwave analysis - A contribution for operando monitoring of gas drying by adsorption. Sensors and Actuators B: Chemical, 2021, 335, 129646.	7.8	1
315	Concept study with experimental proof for a new type of detector for gas chromatography. Sensors and Actuators B: Chemical, 2021, 346, 130490.	7.8	1
316	Gas evolution in electrochemical flow cell reactors induces resistance gradients with consequences for the positioning of the reference electrode. RSC Advances, 2021, 11, 28189-28197.	3.6	1
317	CO Gas Detection on Ptâ^£YSZâ^£Pt Solid Electrolyte Sensors by Methods Based on Dynamic Voltage Variations. Journal of the Electrochemical Society, 2021, 168, 117506.	2.9	1
318	Mikrowellengestützte Systeme zur Zustandserkennung von Abgaskatalysatoren und Abgasfiltern im Überblick. , 2016, , 115-132.		1
319	Optimization of a sensor for a Tian–Calvet calorimeter with LTCC-based sensor discs. Journal of Sensors and Sensor Systems, 2016, 5, 381-388.	0.9	1
320	A Glass Platelet Coating on Battery Electrodes and Its Use as a Separator for Lithium-Ion Batteries. Journal of Electrochemical Energy Conversion and Storage, 2020, 17, .	2.1	1
321	Influence of Pt paste and the firing temperature of screen-printed electrodes on the NO detection by pulsed polarization. Journal of Sensors and Sensor Systems, 2020, 9, 293-300.	0.9	1
322	Mobile sealing and repairing of damaged ceramic coatings by powder aerosol deposition at room temperature. Open Ceramics, 2022, 10, 100253.	2.0	1
323	Miniaturized ceramic differential scanning calorimeter with integrated oven and crucible in LTCC technology. Procedia Engineering, 2010, 5, 940-943.	1.2	0
324	Gas Sensitivity of Pillared and Non-pillared Layered Silicates. Zeitschrift Fur Anorganische Und Allgemeine Chemie, 2010, 636, 2112-2112.	1.2	0

#	Article	IF	CITATIONS
325	Solid-state potentiometric CO <inf>2</inf> -sensor in thick film technology for breath analysis. , 2011, ,		0
326	Cumulative Measurement Principle For The Detection Of Small Amounts Of Gaseous Species. , 2011, , .		0
327	Investigation of Oxygen Reactions in a Screenprinted Pt/YSZ-Model Electrode System. ECS Transactions, 2014, 58, 37-43.	0.5	0
328	FEM-based Modeling of the Temperature Distribution Influence on Melting Process in Ceramic Differential Micro-calorimeter. Procedia Engineering, 2014, 87, 412-415.	1.2	0
329	First Approaches to Integrate a Strain Gauge-Based Mass Detection System into a Miniaturized DSC-device. Procedia Engineering, 2015, 120, 116-119.	1.2	0
330	Singleâ€Crystal Structure and Electronic Conductivity of Melt Synthesized Feâ€rich, near Endâ€Member Ferroâ€Kinoshitalite. Zeitschrift Fur Anorganische Und Allgemeine Chemie, 2017, 643, 1661-1667.	1.2	0
331	Direct Catalyst Conversion Sensor in Form of a Single Self-Heated Mixed-Potential Device. Proceedings (mdpi), 2017, 1, .	0.2	0
332	Planar Microstrip Ring Resonator Structure for Gas Sensing and Humidity Sensing Purposes. Proceedings (mdpi), 2017, 1, 414.	0.2	0
333	2D SnS2—A Material for Impedance-Based Low Temperature NOx Sensing?. Proceedings (mdpi), 2017, 1, .	0.2	0
334	Effect of Ambient Conditions on the Resistance of Metal Oxides as a Novel Material for Outer Corona Protection Systems. , 2018, , .		0
335	Aerosol Deposition Method - A Promising Novel Method to Produce Ceramic Gas Sensor Films at Room Temperature. , 2019, , .		0
336	Novel Concept for Room Temperature NO2 Detection: Using Metal Oxides as Resistive Gas Dosimeters. , 2019, , .		0
337	Beladungsregelung eines NH3-SCR-Katalysator-Systems auf minimale NOx-Emissionen mittels Hochfrequenzsensorik. , 2018, , 225-244.		0